

# Determining novel candidate anti-hepatocellular carcinoma drugs using interaction networks and molecular docking between drug targets and natural compounds of SiNiSan

Qin Zhang<sup>Equal first author, 1</sup>, Zhangying Feng<sup>Equal first author, 2</sup>, Mengxi Gao<sup>1</sup>, Liru Guo<sup>Corresp. 1</sup>

<sup>1</sup> The Fourth Hospital of Hebei Medical University, Department of General Medicine, Shijiazhuang, Hebei, China

<sup>2</sup> The Fourth Hospital of Hebei Medical University, Department of Clinical Pharmacology, Shijiazhuang, Hebei, China

Corresponding Author: Liru Guo  
Email address: qkglrdoctor@126.com

**Background:** SiNiSan (SNS) is an ancient traditional Chinese medicine (TCM) used to treat liver and spleen deficiencies. We studied the unique advantages of using SNS to treat hepatocellular carcinoma (HCC) with multiple components and targets to determine its potential mechanism of action. **Methods:** The active compounds from the individual herbs in the SNS formula and their targets were mined from Traditional Chinese Medicine Systems Pharmacology Database (TCMSP). HCC-associated targets were collected from the TCGA and GEO databases and samples were collected from patients with stage III hepatocellular carcinoma. A compound-disease target network was constructed, visualized, and analyzed using Cytoscape software. We built a protein-protein interaction (PPI) network using the String database. We enriched and analyzed key targets using GSEA, GO, and KEGG in order to explore their functions. Autodock software was used to simulate the process of SNS molecules acting on HCC targets. **Results:** 113 candidate compounds were taken from SNS, and 64 of the same targets were chosen from HCC and SNS. The predominant targets genes were PTGS2, ESR1, CHEK1, CCNA2, NOS2 and AR; kaempferol and quercetin from SNS were the principal ingredients in HCC treatment. The compounds may work against HCC due to a cellular response to steroid hormones and histone phosphorylation. The P53 signaling pathway was significantly enriched in the gene set GSEA enrichment analysis and differential gene KEGG enrichment analysis.

**Conclusions:** Our results showed that the SNS component has a large number of stage III HCC targets. Among the targets, the sex hormone receptors, the AR and ESR1 genes, are the core targets of SNS component and the most active proteins in the PPI network. In addition, quercetin, which has the most targets, can act on the main targets (BAX, CDK1, CCNB1, SERPINE1, CHEK2, and IGFBP3) of the P53 pathway to treat HCC.

1 **Determining novel candidate anti-hepatocellular carcinoma drugs using interaction**  
2 **networks and molecular docking between drug targets and natural compounds of SiNiSan**

3

4

5 Qin Zhang <sup>1,Δ</sup>, Zhangying Feng <sup>2,Δ</sup>, Mengxi Gao <sup>1</sup>, Liru Guo <sup>1\*</sup>

6

7

8 <sup>1</sup> The Fourth Hospital of Hebei Medical University, Department of General Medicine,

9 Shijiazhuang, Hebei, China

10 <sup>2</sup> The Fourth Hospital of Hebei Medical University, Department of Clinical Pharmacology,

11 Shijiazhuang, Hebei, China

12

13

14 <sup>Δ</sup> These authors contribute equally in this work.

15

16

17 Corresponding Author:

18 Liru GUO

19 12 Health Road, Shijiazhuang, Hebei, 050011, China

20 Email address: qkglrdoctor@126.com

21

22

23

24

25

26

27

28

## 29 **Abstract**

30 **Background:** SiNiSan (SNS) is an ancient traditional Chinese medicine (TCM) used to treat  
31 liver and spleen deficiencies. We studied the unique advantages of using SNS to treat  
32 hepatocellular carcinoma (HCC) with multiple components and targets to determine its potential  
33 mechanism of action.

34 **Methods:** The active compounds from the individual herbs in the SNS formula and their targets  
35 were mined from Traditional Chinese Medicine Systems Pharmacology Database (TCMSP).  
36 HCC-associated targets were collected from the TCGA and GEO databases and samples were  
37 collected from patients with stage III hepatocellular carcinoma. A compound-disease target  
38 network was constructed, visualized, and analyzed using Cytoscape software. We built a protein-  
39 protein interaction (PPI) network using the String database. We enriched and analyzed key  
40 targets using GSEA, GO, and KEGG in order to explore their functions. Autodock software was  
41 used to simulate the process of SNS molecules acting on HCC targets.

42 **Results:** 113 candidate compounds were taken from SNS, and 64 of the same targets were  
43 chosen from HCC and SNS. The predominant targets genes were PTGS2, ESR1, CHEK1,  
44 CCNA2, NOS2 and AR; kaempferol and quercetin from SNS were the principal ingredients in  
45 HCC treatment. The compounds may work against HCC due to a cellular response to steroid  
46 hormones and histone phosphorylation. The P53 signaling pathway was significantly enriched in  
47 the gene set GSEA enrichment analysis and differential gene KEGG enrichment analysis.

48 **Conclusions:** Our results showed that the SNS component has a large number of stage III HCC  
49 targets. Among the targets, the sex hormone receptors, the AR and ESR1 genes, are the core  
50 targets of SNS component and the most active proteins in the PPI network. In addition,  
51 quercetin, which has the most targets, can act on the main targets (BAX, CDK1, CCNB1,  
52 SERPINE1, CHEK2, and IGFBP3) of the P53 pathway to treat HCC.

53

## 54 **Introduction**

55 Hepatocellular carcinoma (HCC) is an extremely malignant type of tumor that accounts for the  
56 majority of primary liver cancer cases worldwide. The increased incidence rate of HCC makes it  
57 the leading cause of death among patients with cirrhosis (Forner et al., 2018). Liver cancer is the

58 sixth most common neoplasm and the fourth leading cause of cancer death according to the  
59 GLOBOCAN 2018 report issued by the International Agency for Research (IARC) (Ferlay et al.,  
60 2019).

61 HCC develops in stages and is caused by a combination of factors. Determining the  
62 molecular mechanisms of HCC is complicated due to the physiological functions of the liver  
63 (Pan et al., 2011). The following mechanisms have been confirmed: activation of proto-  
64 oncogenes, such as N-ras and HBVx (Cheng et al., 2014; Kudo, 2011); inactivation of the tumor  
65 suppressor genes, such as p53, Rb, p21 and PTEN (Sandra & Jean-Charles, 2020; Maheshkumar  
66 et al., 2019); abnormal activation of multiple molecular signaling pathways; and the expression  
67 of HCC-associated proteins. HCC treatments focus on increasing survival while maintaining a  
68 high quality of life. The treatments include surgery, interventional therapy, chemotherapy, and  
69 combination therapy. Surgical treatments include hepatectomy, liver transplantation, and local  
70 ablative therapies. However, these are only used for early-stage liver cancer and tumors that are  
71 localized and not metastasized (Villanueva, 2019). Vascular interventional therapy mainly  
72 consists of transarterial chemoembolization (TACE) and transcatheter arterial infusion (TAI),  
73 which can effectively control the growth of HCC cells. However, there is no standardized staging  
74 or guidelines for interventional therapy ischemia, and hypoxia in tumor tissues after TACE  
75 therapy may lead to the increase of hypoxia-inducible factors, resulting in the high expression of  
76 VEGF in residual tumors, and eventually causing cancer recurrence and metastasis.

77 Chemotherapy is an important option for HCC treatment but is limited by its toxic side effects.  
78 An effective systematic treatment is required for patients with terminal-stage liver cancer or  
79 patients with severe underlying disease to act on multiple mechanisms and control tumor  
80 progression (Grandhi et al., 2016). Tumor staging is a crucial step in the treatment of HCC. TNM  
81 (Tumour, Node, Metastasis) and BCLC (The Barcelona Clinic Liver Cancer) are currently the  
82 most widely used evaluation systems, combined with the HCC study published in the Lancet in  
83 2018 and the 2016 version of the AASLD (American Association for the Study of Liver  
84 Diseases) guideline (Forner et al., 2018; Heimbach et al., 2018). Patients with early stage HCC  
85 that tumor diameters  $\leq 5$ cm (T1, T2 or BCLC0, BCLCA) can benefit from resection,  
86 transplantation, and ablation treatments, for advanced HCC, the selection of treatment type  
87 depends on the extent of invasion of macrovascular, metastasis, and the physical condition of the  
88 patient, systemic treatment and the best supportive care may be the best choice, and this is

89 exactly what we hope TCM achieves. Therefore, this study selected stage III hepatocellular  
90 carcinoma as samples for follow-up research.

91 Traditional Chinese medicine (TCM) refers to medicines used in China for thousands of years;  
92 they are typically derived from different natural medicines and herbal products and have made  
93 significant contributions to human health (Tao et al., 2015; Hao et al., 2017; Cheng et al., 2019;  
94 Xiao-Cong et al., 2018). Advances in analytical technologies and methodologies have  
95 accelerated the research of TCM, and the role of TCM in anti-tumor alternative therapies has  
96 received increasing attention (Lee et al., 2019). Studies have confirmed that TCM is effective in  
97 improving the survival rate of patients with breast and lung cancers (Lee et al., 2014; Hsiao &  
98 Liu, 2010; Liao et al., 2017). SiNiSan (SNS) is a basic TCM formulation and was first  
99 introduced in the Treatise on Febrile Disease by Zhang Zhongjing, a famous physician in the late  
100 eastern Han Dynasty. SNS consists of 4 herbs: Gancao (Radix Glycyrrhizae), Chaihu (Radix  
101 Bupleuri), Zhishi (Fructus Aurantii Immaturus), and Baishao (Radix Paeoniae Alba). It is used  
102 for treating liver stagnation and spleen deficiency, improving disorders of the digestive system,  
103 and alleviating depression (Jiang et al., 2003). Studies have confirmed that SNS can affect the  
104 invasiveness and metastatic potential of hepatocellular carcinoma cells by inhibiting the  
105 phosphorylation of extracellular signal-related kinases and c-Jun N-terminal kinase signaling  
106 pathway (Hung-Jen et al., 2015). The mechanism is unclear, which has limited its clinical  
107 applications, thus, the therapeutic effects of SNS on hepatocellular carcinoma needs to be  
108 determined. Network pharmacology (NP) is an emerging drug research strategy that places the  
109 effects of drugs on diseases in a complex biological network and uses related gene databases to  
110 determine the mechanism of action of the drug compounds (Zhang et al., 2019). NP has  
111 accelerated pharmacological development and improved our understanding of mechanisms of  
112 drug action by establishing a multi-layer network of disease-phenotype-gene-drug (Xiao-Ming &  
113 Chun-Fu, 2015) and is an important application for TCM research.

114 We downloaded the active pharmaceutical ingredients and target genes of SNS from the  
115 TCMSp database and obtained the disease genes of stage III hepatocellular carcinoma (HCC)  
116 from the TCGA and GEO databases. Gene Set Enrichment Analysis (GSEA) enrichment  
117 analysis was conducted on the gene sets of the two databases, and differential analysis was  
118 conducted to screen out the HCC genes with significant differences. The compound-disease  
119 target network was obtained from the intersection of the SNS targets and the HCC differential

120 genes. The possible mechanisms and pathways of SNS were studied by analyzing the active  
121 compounds of SNS in the network, performing GO and KEGG enrichment analysis on the  
122 intersected genes, and constructing a protein interaction network. Finally, we used molecular  
123 docking to simulate the process of SNS active molecules acting on target HCC genes. We  
124 investigated the bioactive compounds, crossing targets, and possible mechanisms of SNS on  
125 hepatocellular carcinoma using a network pharmacology strategy to provide new theoretical  
126 treatments.

127

## 128 **Materials & Methods**

### 129 **Screening of bioactive compounds and targets in SiNiSan**

130 The individual herbs and active components (Radix Glycyrrhizae, Radix Bupleuri, Fructus  
131 Aurantii Immaturus and Radix Paeoniae Alba) in SNS were mined from the Traditional Chinese  
132 Medicine Systems Pharmacology Database (TCMSP: <http://tcmospw.com/tcmosp.php/>). This  
133 database contains the active ingredients of Chinese medicine and their corresponding targets  
134 (Yang et al., 2019). Herbal medicines are screened by TCMSP based on absorption, distribution,  
135 metabolism, and excretion (ADME) and includes factors like oral bioavailability (OB), drug-  
136 likeness (DL), and P450 (Lee et al., 2019). OB represents the speed and degree of drug  
137 absorption in the circulation and DL represents the similarity between the herbal ingredients and  
138 specific medicines, suggesting that herbs may be used as therapeutic agents. Refer to TCMSP's  
139 platform research and related traditional Chinese medicine research in the past (Jinlong et al.,  
140 2014; Xue et al., 2012), we selected OB and DL as conditions and set the filter criteria to  
141  $OB \geq 30\%$  and  $DL \geq 0.18$  for potential bioactive compounds by Strawberry-perl software  
142 (<https://www.perl.org>, ver.5.30.1.1).

### 143 **Prediction and Gene Set Enrichment Analysis (GSEA) enrichment analysis of stage III** 144 **hepatocellular carcinoma targets**

145 HCC-associated targets were acquired from The Cancer Genome Atlas (TCGA) and Gene  
146 Expression Omnibus (GEO). TCGA is a collaborative database from the National Cancer  
147 Institute (NCI) and the National Human Genome Institute (NHGRI), which is responsible for a  
148 large amount of clinical and genomic data for various cancer types. The GEO database is an  
149 international public gene expression database affiliated with NCBI that covers sufficient disease-

150 differential genes profiling by array (Barrett et al., 2013). TCGA data were obtained from the  
151 GDC Data Portal (<https://portal.gdc.cancer.gov/>), select the TCGA-LIHC (Liver Hepatocellular  
152 Carcinoma) project in the liver cancer classification, pick and summarize the stage III  
153 hepatocellular carcinoma cases as the disease Group, and the normal adjacent tissues in HCC  
154 cases as the normal group. Similarly, search for HCC data in the GEO database  
155 (<https://www.ncbi.nlm.nih.gov/>) with "hepatocellular carcinoma" and "normal" as keywords, and  
156 set the conditions as Homo sapiens to obtain a set of HCC gene expression profiles  
157 (GSE101685) and its RNA chip annotation files (GPL570), then based on the annotation file, use  
158 Strawberry-perl-5.30.1.1 software to convert the chip probe ID into gene symbol, and selected  
159 the HCC samples of stage III as the disease group, and the normal tissue samples as the normal  
160 group. GSEA calculated the results of the overall pathway or function enrichment through  
161 enrichment analysis of the gene sets that did not undergo differential analysis nor did it interfere  
162 with artificially set thresholds, which is to determine whether the predefined gene set can show a  
163 consistent enrichment trend in overall genes include the disease group and the normal group. In  
164 order to perform GSEA analysis, the above-mentioned GEO and TCGA gene data were sorted  
165 into a matrix file which includes the disease group and the normal group. We selected the  
166 Canonical pathways of the C2 curated gene sets (c2.cp.pid.v7.1) in the Molecular Signatures  
167 Database (MSigDB) and analyzed them using GSEA software (ver 4.0.3).

### 168 **Differential analysis of stage III hepatocellular carcinoma targets and the building of a** 169 **compound-disease target network**

170 Analyzing the HCC sample genes and normal sample genes from TCGA and GEO, and get the  
171 differentially expressed genes (DEGs) that are significantly different from the normal group in  
172 the disease group. DEGs for stage III HCC were obtained by limma package in R software  
173 (<https://www.r-project.org/>, ver 3.6.2) based on two criteria ( $|\log_{2}FC| > 1$  and  $\text{adj.P Value} < 0.05$ ).  
174 The duplicates were removed after obtaining the differential genes from the TCGA and GEO  
175 databases. We determined the intersection of the SNS bioactive drug targets and DEGs of HCC  
176 using Strawberry-perl-5.30.1.1 software to obtain the targets for compound-disease network. The  
177 compound-disease target network was built, visualized, and analyzed using Cytoscape software  
178 (<https://cytoscape.org/>, ver3.7.2). The nodes in the network indicated the HCC target genes and  
179 the SNS bioactive compounds. The edges indicated their interactions.

### 180 **Protein-protein interaction (PPI) network**

181 The protein-protein interaction (PPI) network was constructed using the string database  
182 (<https://string-db.org/>) based on crossing targets that determined the interactions between gene  
183 regulatory proteins. The string database contains a large amount of protein interaction  
184 information from experiments or other databases and can predict the mode of action between  
185 HCC-related proteins. We entered 64 intersection HCC genes, selected the species as Homo  
186 sapiens, and set the minimum required interaction score to 0.4 (default) to set up a PPI network.  
187 The active protein interaction sources included text mining, experiments, databases, co-  
188 expressions, neighborhoods, gene fusions, and co-occurrence. We imported the network to  
189 Cytoscape for node and connection analyses.

### 190 **GO and KEGG pathway enrichment analysis**

191 We conducted Gene Ontology (GO) and Kyoto Encyclopedia of Genes and Genomes (KEGG)  
192 enrichment analysis of 64 HCC target genes to clarify the biological functions and pathways of  
193 SNS compounds for treating HCC. GO enrichment analysis included the biological process (BP)  
194 and cell compounds (CC). GO and KEGG enrichment analysis ( $P \leq 0.05$ ,  $Q \leq 0.05$ ) were conducted  
195 using the bioconductor package in R software (ver3.6.2).

### 196 **Molecular docking to simulate the core target-compound binding**

197 We downloaded the PDB file of targets from the RCSB PDB website  
198 (<https://www.rcsb.org/#Category-search>) and the MOL2 file of the compound ligand from the  
199 ZINC database (<http://zinc.docking.org/>) and selected a target related to HCC and performed  
200 molecular docking with the corresponding compound. We used the AutoDock software  
201 (ver4.2.6) to dehydrate and hydrogenate the macromolecules. We calculated the charge of the  
202 target macromolecular protein, determined the rotation bond of the ligand, selected the  
203 macromolecule, set the box, ran Autogrid to make the macromolecular crystal structure, and ran  
204 Autodock to create a rigid docking of the macromolecules and ligands. The docking algorithm  
205 was set as the local search parameter using Python 2.5 and we used Pymol software (ver2.3.4) to  
206 perform the visualization of the docking result.

207

## 208 **Results**

### 209 **Bioactive compounds and targets in SiNiSan**

210 A total of 779 compounds and 6984 targets in SNS were collected from TCMSP. We obtained  
211 92 bioactive compounds and 1769 targets in Radix Glycyrrhizae, 17 bioactive compounds and  
212 123 targets in Radix Bupleur, 22 bioactive compounds and 348 targets in Fructus Aurantii  
213 Immaturus, 13 bioactive compounds and 306 targets in Radix Paeoniae Alba with 21 repeat  
214 compounds after screening by  $OB \geq 30\%$  and  $DL \geq 0.18$ . 113 compounds were identified as  
215 potential bioactive molecules for further study.

### 216 **Hepatocellular carcinoma-associated targets and GSEA enrichment analysis results**

217 The genetic data from the TCGA database included 47 stage III hepatocellular tumor samples  
218 and 7 and normal adjacent tissue samples. The dataset (GSE101685) selected from the GEO  
219 database had 24 samples including 8 control (normal) samples and 16 test (stage III HCC)  
220 samples. The results of GSEA enrichment analysis of the HCC gene sets in the two databases  
221 showed that the stage III hepatocellular carcinoma group from TCGA was significantly enriched  
222 in 82 pathways (nominal p value  $< 0.05$  and FDR  $< 25\%$ ), sorted by their normalized enrichment  
223 score (NES). The pathways with the highest enrichment levels are shown in Figure 1. The stage  
224 III hepatocellular carcinoma group from GEO was significantly enriched in 9 pathways (nominal  
225 p value  $< 0.05$  and FDR  $< 25\%$ ), as shown in Figure 2. The enrichment bar plot of the genes in the  
226 two databases are shown in Figure 3. Based on the above results, all 9 pathways enriched in the  
227 HCC gene set from GEO are also enriched in the TCGA data. HCC genes were significantly  
228 enriched in the ATR, FANCONI, AURORA\_B, PLK1, ARF3, MTOR4, P53\_REGULATION,  
229 LKB1, ATM, and E2F pathways. All of these pathways are upregulated in HCC.

230 2569 differential genes were obtained after differential analysis including 1614 up-regulated  
231 genes and 955 down-regulated genes from TCGA. We obtained 1078 differential genes,  
232 including 370 up-regulated genes and 708 down-regulated genes from GEO. Differential  
233 expression genes of TCGA and GEO are shown in a volcano map (Figure 4).

### 234 **Analysis of compound-disease target network**

235 A total of 3101 HCC differential genes were obtained after synthesizing the differential genes of  
236 the two databases and removing the duplicates. 64 HCC target genes were obtained through the  
237 intersection of SNS targets and HCC differential genes. We built a visualized compound-disease  
238 target network by combining these with 113 bioactive compounds that had been previously  
239 obtained (Figure 5). 177 nodes and 610 edges are shown in the network. Most SNS molecules  
240 can act on multiple HCC targets, the most predominant of which is quercetin (MOL000098) with

241 40 edges, followed by kaempferol (MOL000422) with 17 edges. Table 1 shows the 30 most  
242 prevalent ingredients in SNS prescriptions that act on the largest number of HCC targets. PTGS2  
243 (106 edges), ESR1 (84 edges), AR (74 edges), NOS2 (74 edges), CCNA2 (53 edges) and  
244 CHEK1 (50 edges) are the genes regulated by at least 1 compound. The target gene linkage  
245 is >50 degrees, indicating that these targets might be a key target for SNS treatment of HCC.

#### 246 **Analysis of protein-protein interactions (PPI) network**

247 The protein interactions of HCC differential genes extracted from the human genome were  
248 shown in the PPI network (Figure 6). Each node in the network diagram represents a target gene,  
249 the connection between the nodes indicates that there is an interaction relationship, and the color  
250 of the nodes changing from blue to red represents the degree of the nodes changing from low to  
251 high. The overall network included 64 nodes and 343 edges (PPI enrichment p-value: <1.0e-16),  
252 the average node degree was 10.7 and the genes with the highest node degrees are: ESR1 (31  
253 edges), MYC (30 edges), JUN (30 edges), FOS (25 edges), CAT (24 edges), and AR (22 edges).

#### 254 **GO and KEGG pathway enrichment analysis**

255 The results of GO enrichment analysis of the 64 HCC target genes showed that the effect of SNS  
256 on HCC may be mainly associated with the response to factors including metal ion, cadmium ion,  
257 oxidative stress, steroid hormone, histone phosphorylation, cyclin-dependent protein kinase  
258 holoenzyme complex, RNA polymerase II transcription factor complex, and the chromosomal  
259 region. The distribution of enrichment results is shown in Figure 7. According to KEGG  
260 enrichment analysis of HCC target genes, the major pathways for herbal interventions in HCC  
261 are the p53 signaling pathway (hsa04115), calcium signaling pathway (hsa04020), NF-kappa B  
262 signaling pathway (hsa04064), and the HIF-1 signaling pathway (hsa04066). The enrichment  
263 results of KEGG pathways are shown in Table 2.

#### 264 **Docking results of compound and core target**

265 Our results showed that quercetin can act on the greatest number of HCC targets. Therefore, we  
266 docked the core targets involved in the component disease network (AR, BAX, CHEK2, ESR1,  
267 NOS2, PTGS2) with quercetin (Figure 5). We downloaded the PDB files of the HCC targets and  
268 the Mol2 files of the ligand quercetin (ZINC6484693) for docking. The quercetin structure has 6  
269 rotatable bonds and the hydrogen bond binding energy, total internal energy, and electrostatic  
270 energy are distinct due to its position and the different positions of the amino acid fragments of  
271 the target protein. The docking results of the quercetin ligand, the HCC target macromolecule,

272 the hydrogen bond binding energy, total internal energy, and electrostatic energy are shown in  
273 Table 3. The inhibition constant is the dissociation constant of the protein-inhibitor complex and  
274 the inhibition constant is smaller as the inhibition strength increases. The molecular docking of  
275 CHEK2, BAX, AR, PTGS2 and quercetin are shown in Figure 8.

276

## 277 Discussion

278 HCC arises from hepatocytes in the liver parenchyma and is typically seen in patients with  
279 chronic liver disease, including viral hepatitis, alcoholic liver disease, and nonalcoholic fatty  
280 liver disease (Arslanoglu et al., 2016). Hepatocarcinogenesis is a multi-factorial process with  
281 various signaling pathways that include the p53 signaling pathway, VEGF signaling pathway,  
282 TGF signaling pathway, and Ras MARK signaling pathway (Grandhi et al., 2016). 75% of  
283 patients with limited stage cancer have a survival rate of approximately 5 years when treated  
284 with curative therapies such as liver transplantation and surgical resection (Guy et al., 2012).  
285 However, for patients in hepatic decompensation or with a highly heterogeneous tumor, surgery  
286 is not always effective and has a significant economic burden on patients. HCC is resistant to  
287 chemotherapy, thus an alternative treatment must be established.

288 TCM is prepared according to the principle of “King, Vassal, Assistant, and Delivery servant”  
289 based on the patient’s disease state (Zhang et al., 2019). This principle determines the major  
290 therapeutic compounds combined with other agents used to restore the balance of body functions  
291 and reduce toxicity, which can be exhibited in symptoms including insomnia, palpitation,  
292 infections, and fever (Li et al., 2020). Studies have found that TCM plays an anti-tumor role  
293 through apoptotic pathways in ROS-mediated mechanisms, DNA damage-mediated mechanisms,  
294 Ca<sup>2+</sup>-mediated mechanisms, and by blocking transcription or translation (Min, 2010). TCM  
295 inhibits cell proliferation and promotes the apoptosis of tumor cells by targeting the stimulation  
296 of the host immune response for cytotoxic activity (Liao et al., 2015; Zhao et al., 2018). SNS has  
297 been used for centuries in China as a remedy for liver stagnation and spleen deficiencies. Recent  
298 experiments have shown that SNS is a remarkably effective treatment for hepatitis and liver  
299 injury (Shu et al., 2018). The individual herbs that make up SNS have anti-inflammatory, anti-  
300 bacterial, anti-oxidation, anti-tumor, anti-proliferation, anti-angiogenic, anti-HBV, and apoptotic  
301 effects in vitro and in vivo (Zhao et al., 2018; Li et al., 2020; Ma et al., 2014; Sun et al., 2019;  
302 Xiang et al., 2019; Pan et al., 2019); Zhou et al., 2019; Lefaki et al., 2020).

303 In our research, there are 64 overlaps between drug targets and disease targets which are the  
304 important targets involved in the therapeutic mechanism of SNS, we studied 113 compounds and  
305 64 target genes using the screening criteria and found that each bioactive compound acts on at  
306 least 1 HCC differential gene, core targets genes were PTGS2, ESR1, AR, NOS2, CCNA2 and  
307 CHEK1. The majority of the compounds were derived from Radix Glycyrrhizae (Gancao), which  
308 indicated that Radix Glycyrrhizae may be the principal active herb in treating HCC. Radix  
309 Bupleuri, Fructus Aurantii Immaturus, and Radix Paeoniae Alba may play a supporting role.  
310 Quercetin and kaempferol are bioactive ingredients with the highest number of targets and both  
311 coexist in multi-herb formulations (quercetin from Radix Glycyrrhizae and Radix Bupleuri,  
312 kaempferol from Radix Glycyrrhizae, Radix Bupleuri and Radix Paeoniae Alba). In order to  
313 study the molecular mechanism of disease development from a systematic perspective, we  
314 constructed a PPI network to predict the mode of action between HCC-related proteins and to  
315 provide a reference for the role of drugs. AR and ESR1 were found to be the targets that interact  
316 with the most proteins in the PPI network and also act as targets for a large number of drug  
317 components. This suggests that AR and ESR1 may be important nodes for SNS to act on HCC.  
318 AR is an androgen receptor involved in the growth and progression of hepatocellular carcinoma,  
319 it can inhibit the expression of CD90 in circulating tumor cells by up-regulating histone 3H2A  
320 (Han et al., 2020). Targeting the AR transduction pathway may be the key to inhibiting the  
321 progression of advanced HCC (Han et al., 2020; Ma et al., 2014). ESR1 is an estrogen receptor  
322 that causes abnormal serum methylation and can be used as a biomarker for the diagnosis of  
323 HCC. The imbalance of ESR1 expression can cause a high degree of HCC amplification  
324 (Tsiambas et al., 2011; Dou et al. 2016) and is a focus of targeted therapy.

325 Enrichment analysis revealed that these compounds may act against HCC through: the  
326 cellular response to steroid hormones; oxidative stress; histone phosphorylation; steroid  
327 metabolic processes; cyclin-dependent protein kinase holoenzyme complex; synthesis of RNA  
328 polymerase II transcription factor complex and the nuclear transcription factor complex. The  
329 response of these biological functions on steroid hormones coincided with the target AR and  
330 ESR1, suggesting that SNS may regulate the levels of sex hormones. Histone H3  
331 phosphorylation is involved in the chemical carcinogenesis of HCC, while histone 4  
332 phosphorylation is related to the proliferation and differentiation of hepatocytes after a liver  
333 injury (Sukumar et al., 2020; Liu & Liu, 2020). The potential pathways are: the p53 signaling

334 pathway; calcium signaling pathway; NF-kappa B signaling pathway; and the HIF-1 signaling  
335 pathway. The P53 pathway has the highest degree of enrichment, combined with the previous  
336 gene set GSEA analysis. The P53 pathway is also significantly enriched in the overall stage III  
337 hepatocellular carcinoma gene set. Previous studies have demonstrated that P53 inhibits the  
338 progression, recurrence, and related immune responses of HCC (G et al., 2013; Xiaonian et al.,  
339 2017). The signaling pathway exists in p53 in HCC based on the HCC map in KEGG  
340 (<https://www.kegg.jp>) and acts as tumor suppressor. The SNS target genes in the p53 pathway  
341 include BAX, CDK1, CHEK1, CCNB1, SERPINE1, CHEK2, and IGFBP3. Quercetin interferes with  
342 6 of the 7 target genes in the above-mentioned p53 pathway (BAX, CDK1, CCNB1, SERPINE1,  
343 CHEK2, IGFBP3) and molecular docking confirmed that quercetin can bind to the P53 pathway-  
344 related targets (CHEK2, SPRPINE1, BAX). Thus, quercetin is likely to be a promising HCC  
345 treatment drug in SNS. Quercetin is a bioflavonoid with high antitumor activity that acts on  
346 cancers such as osteosarcoma and colon cancer by rebuilding the tumor microenvironment and  
347 alleviates liver damage by regulating the EGFR pathway (Choi et al., 2010; Lan et al., 2017; Hu  
348 et al., 2017; Carrasco-Torres et al., 2017; Massi et al., 2017), Quercetin can exert anti-tumor  
349 activity by targeting HSP70/90, P13K, and NF-B and has been reported in the treatment of  
350 hepatocellular carcinoma (Fernández, F.P et al., 2019; Wang R. E et al 2011 ). Our other derived  
351 pathways require testing to determine their efficacy in the treatment of HCC.

352

## 353 **Conclusions**

354 TCM assumes the characteristics of multiple compounds, targets and pathways when applied to  
355 disease prevention and treatment, which is the focus of network pharmacology. We predicted the  
356 targets and potential mechanisms of SNS compounds for HCC treatment by constructing  
357 networks and used molecular docking to simulate their behavior. We focused on quercetin's  
358 targeting of genes that were enriched in the p53 pathway and then inhibited the progression of  
359 HCC by regulating the p53 pathway. GSEA enrichment analysis of the HCC gene set and the  
360 KEGG enrichment analysis of the intersection gene after the differential analysis show that the  
361 P53 pathway is a pathway with significant influence. AR and ESR1 in HCC targets are also  
362 worthy of attention due to their large number of SNS components and the proteins that are highly  
363 interactive with other proteins in the PPI network. Research has revealed that these two sex

364 hormone receptors are involved in the development of HCC. SNS can inhibit HCC by affecting  
365 hormone levels and by regulating the P53 pathway. The results of this study should be verified  
366 by in vivo and vitro experiments and more studies are needed to reduce the toxicity of TCM and  
367 prove its value in the treatment of HCC.

368

## 369 **Acknowledgements**

370 We would like to thank Professor Helin Feng for the research guidance and technical support of  
371 this study.

372

## 373 **References**

- 374 Arslanoglu, A., Seyal, A.R., Sodagari, F., Sahin, A., Miller, F.H., Salem, R., and Yaghmai, V.  
375 2016. Current Guidelines for the Diagnosis and Management of Hepatocellular Carcinoma: A  
376 Comparative Review. *AJR. American journal of roentgenology* 207:W88.
- 377 Barrett, T., Wilhite, S.E., and Ledoux, P. 2013. NCBI GEO: archive for functional genomics data  
378 sets--update. *NUCLEIC ACIDS RESEARCH* 41.
- 379 Carrasco-Torres, G., Monroy-Ramírez, H.C., Martínez-Guerra, A.A., Baltiérrez-Hoyos, R.,  
380 Romero-Tlalolini, M.D.L.Á., Villa-Treviño, S., Sánchez-Chino, X., and Vásquez-Garzón, V.R.  
381 2017. Quercetin Reverses Rat Liver Preneoplastic Lesions Induced by Chemical Carcinogenesis.  
382 *Oxidative Medicine and Cellular Longevity* 2017. 10.1155/2017/4674918
- 383 Cheng, X., Wence, Z., Yuming, W., and Liang, Q. 2014. Hepatitis B virus-induced  
384 hepatocellular carcinoma. *Cancer Letters* 345:216-222.
- 385 CHENG, X.R., QI, C.H., and WANG, T.X. 2019. Characteristics of the traditional Liu-Wei-Di-  
386 Huang prescription reassessed in modern pharmacology. *Chinese Journal of Natural Medicines*  
387 17:103-121.
- 388 Choi, K.C., Chung, W.T., Kwon, J.K., Yu, J.Y., Jang, Y.S., Park, S.M., Lee, S.Y., and Lee, J.C.  
389 2010. Inhibitory effects of quercetin on aflatoxin B1-induced hepatic damage in mice. *FOOD*  
390 *AND CHEMICAL TOXICOLOGY* 48:2747-2753. 10.1016/j.fct.2010.07.001

- 391 Dou CY., Fan YC., Cao CJ., Yang Y., Wang K. 2016. Sera DNA Methylation of CDH1,  
392 DNMT3b and ESR1 Promoters as Biomarker for the Early Diagnosis of Hepatitis B Virus-  
393 Related Hepatocellular Carcinoma. *Digestive Diseases and Sciences* 61: 1130-1138.  
394 [10.1007/s10620-015-3975-3](https://doi.org/10.1007/s10620-015-3975-3)
- 395 Ferlay, J., Colombet, M., Soerjomataram, I., Mathers, C., Parkin, D.M., Piñeros, M., Znaor, A.,  
396 and Bray, F. 2019. Estimating the global cancer incidence and mortality in 2018: GLOBOCAN  
397 sources and methods. *INTERNATIONAL JOURNAL OF CANCER* 144:1941-1953.  
398 [10.1002/ijc.31937](https://doi.org/10.1002/ijc.31937)
- 399 Forner, A., Reig, M., and Bruix, J. 2018. Hepatocellular carcinoma. *LANCET* 391:1301-1314.
- 400 G, P., Besant, P.V., and Attwood. 2013. Histone H4 histidine phosphorylation: kinases,  
401 phosphatases, liver regeneration and cancer. *BIOCHEMICAL SOCIETY TRANSACTIONS*  
402 40:290-293.
- 403 Grandhi, M.S., Kim, A.K., Ronnekleiv-Kelly, S.M., Kamel, I.R., Ghasebeh, M.A., and Pawlik,  
404 T.M. 2016. Hepatocellular carcinoma: From diagnosis to treatment. *Surgical Oncology* 25:74-85.  
405 [10.1016/j.suronc.2016.03.002](https://doi.org/10.1016/j.suronc.2016.03.002)
- 406 Guy, J., Kelley, R.K., Roberts, J., Kerlan, R., Yao, F., and Terrault, N. 2012. Multidisciplinary  
407 Management of Hepatocellular Carcinoma. *Clinical Gastroenterology and Hepatology* 10:354-  
408 362. [10.1016/j.cgh.2011.11.008](https://doi.org/10.1016/j.cgh.2011.11.008)
- 409 Han Q., Yang D., Yin C., Zhang J. Androgen Receptor (AR)-TLR4 Crosstalk Mediates Gender  
410 Disparities in Hepatocellular Carcinoma Incidence and Progression. *Journal of Cancer* 11: 1094-  
411 1103. [10.7150/jca.30682](https://doi.org/10.7150/jca.30682)
- 412 Hao, P., Jiang, F., Cheng, J., Ma, L., Zhang, Y., and Zhao, Y. 2017. Traditional Chinese  
413 medication for cardiovascular disease. *JOURNAL OF THE AMERICAN COLLEGE OF*  
414 *CARDIOLOGY* 69.
- 415 Hsiao, W.L.W., and Liu, L. 2010. The Role of Traditional Chinese Herbal Medicines in Cancer  
416 Therapy – from TCM Theory to Mechanistic Insights. *PLANTA MEDICA* 76.
- 417 Hu, K., Miao, L., Goodwin, T.J., Li, J., Liu, Q., and Huang, L. 2017. Quercetin Remodels the  
418 Tumor Microenvironment To Improve the Permeation, Retention, and Antitumor Effects of  
419 Nanoparticles. *ACS Nano* 11:4916-4925. [10.1021/acsnano.7b01522](https://doi.org/10.1021/acsnano.7b01522)

- 420 Hung, J.L., Shung, T.K., Yu, M.S., Chia, C.Y. 2015. The Chinese medicine Sini-San inhibits  
421 HBx-induced migration and invasiveness of human hepatocellular carcinoma. *BioMedCentral*  
422 *Complementary and Alternative Medicine* 15:348. [10.1186/1758-2946-6-13](https://doi.org/10.1186/1758-2946-6-13)
- 423 Jiang, J., Zhou, C., Xu, Q., China, P.U., School, O.L.S., ADepartment, O.P.F.C., Nanjing, U.,  
424 and BState, K.L.O.P. 2003. Alleviating Effects of Si-Ni-San, a Traditional Chinese Prescription,  
425 on Experimental Liver Injury and Its Mechanisms. *Biological and Pharmaceutical Bulletin*  
426 26:1089-1094. [10.1248/bpb.26.1089](https://doi.org/10.1248/bpb.26.1089)
- 427 Jinlong, R., Peng, L., Jinan, W., Wei, Z., Bohui, L., Chao, H., Pidong, L., Zihu, G., Weiyang, T.,  
428 Yinfeng, Y., Xue, X., Yan, L., Yonghua, W., Ling Y. 2014. TCMSP: a database of systems  
429 pharmacology for drug discovery from herbal medicines. *Journal of Cheminformatics*, 2014, 6:  
430 13.
- 431 Heimbach, JK., Kulik, LM., Finn, R., Sirlin, CB., Abecassis, M., Roberts, LR., Zhu, A., Murad,  
432 MH., Marrero, J. 2018. AASLD Guidelines for the Treatment of Hepatocellular Carcinoma.  
433 *HEPATOLOGY* 67: 358-380. [10.1002/hep.29086](https://doi.org/10.1002/hep.29086).
- 434 Kudo, M. 2011. Molecular Targeted Therapy for Hepatocellular Carcinoma: Bench to Bedside.  
435 *DIGESTIVE DISEASES -BASEL-* 29.
- 436 Lan, H., Hong, W., Fan, P., Qian, D., Zhu, J., and Bai, B. 2017. Quercetin Inhibits Cell  
437 Migration and Invasion in Human Osteosarcoma Cells. *CELLULAR PHYSIOLOGY AND*  
438 *BIOCHEMISTRY* 43:553-567. [10.1159/000480528](https://doi.org/10.1159/000480528)
- 439 Lee, W., Lee, C., Kim, Y., and Kim, C. 2019. The Methodological Trends of Traditional Herbal  
440 Medicine Employing Network Pharmacology. *Biomolecules* 9:362. [10.3390/biom9080362](https://doi.org/10.3390/biom9080362)
- 441 Lee, Y., Chen, T., Shih, Y.V., Tsai, C., Chang, C., Liang, H., Tseng, S., Chien, S., and Wang, C.  
442 2014. Adjunctive Traditional Chinese Medicine Therapy Improves Survival in Patients With  
443 Advanced Breast Cancer. *CANCER* 120:1338-1344. [10.1002/cncr.28579](https://doi.org/10.1002/cncr.28579)
- 444 Lefaki, M., Papaevgeniou, N., Tur, J.A., Vorgias, C.E., Sykiotis, G.P., and Chondrogianni, N.  
445 2020. The dietary triterpenoid 18 $\alpha$ -Glycyrrhetic acid protects from MMC-induced  
446 genotoxicity through the ERK/Nrf2 pathway. *Redox Biology* 28:101317.  
447 [10.1016/j.redox.2019.101317](https://doi.org/10.1016/j.redox.2019.101317)
- 448 Li, J., Tang, F., Li, R., Chen, Z., Lee, S.M., Fu, C., Zhang, J., and Leung, G.P. 2020. Dietary  
449 compound glycyrrhetic acid suppresses tumor angiogenesis and growth by modulating

450 antiangiogenic and proapoptotic pathways in vitro and in vivo. *The Journal of Nutritional*  
451 *Biochemistry* 77:108268. 10.1016/j.jnutbio.2019.108268

452 Li, L., Qiu, H., Liu, M., and Cai, Y. 2020. A Network Pharmacology-Based Study of the  
453 Molecular Mechanisms of Shaoyao-Gancao Decoction in Treating Parkinson's Disease.  
454 *Interdisciplinary Sciences: Computational Life Sciences*. 10.1007/s12539-020-00359-7

455 Liao, Y., Lin, C., Lai, H., Chiang, J., Lin, J., and Li, T. 2015. Adjunctive traditional Chinese  
456 medicine therapy improves survival of liver cancer patients. *LIVER INTERNATIONAL* 35.

457 Liao, Y.H., Li, C.I., Lin, C.C., Lin, J.G., Chiang, J.H., and Li, T.C. 2017. Traditional Chinese  
458 medicine as adjunctive therapy improves the long - term survival of lung cancer patients. *Journal*  
459 *of Cancer Research and Clinical Oncology* 143:2425-2435. 10.1007/s00432-017-2491-6

460 Liu, X., and Liu, J. 2020. Tanshinone I induces cell apoptosis by reactive oxygen species-  
461 mediated endoplasmic reticulum stress and by suppressing p53/DRAM-mediated autophagy in  
462 human hepatocellular carcinoma. *Artificial Cells, Nanomedicine, and Biotechnology* 48:488-497.  
463 10.1080/21691401.2019.1709862

464 Ma, X., Jin, S., Zhang, Y., Wan, L., Zhao, Y., and Zhou, L. 2014. Inhibitory Effects of Nobiletin  
465 on Hepatocellular Carcinoma In Vitro and In Vivo. *PHYTOTHERAPY*  
466 *RESEARCH* 28:560-567. 10.1002/ptr.5024

467 Maheshkumar, K., Sridharan, J., Kannan, M.R., Chander, C.S., Mathan, G., and Velanganni,  
468 A.A.J. 2019. AEG-1/miR-221 Axis Cooperatively Regulates the Progression of Hepatocellular  
469 Carcinoma by Targeting PTEN/PI3K/AKT Signaling Pathway. *INTERNATIONAL JOURNAL*  
470 *OF MOLECULAR SCIENCES* 20.

471 Massi, A., Bortolini, O., Ragno, D., Bernardi, T., Sacchetti, G., Tacchini, M., and De Risi, C.  
472 2017. Research Progress in the Modification of Quercetin Leading to Anticancer Agents.  
473 *MOLECULES* 22:1270. 10.3390/molecules22081270

474 Ma WL., Lai HC., Yeh S., Cai X., Chang C. 2014. Androgen receptor roles in hepatocellular  
475 carcinoma, fatty liver, cirrhosis and hepatitis. *Endocr. Relat. Cancer* 21:R165-182 [10.1530/ERC-](https://doi.org/10.1530/ERC-13-0283)  
476 [13-0283](https://doi.org/10.1530/ERC-13-0283)

477 Min, L. 2010. Targeting apoptosis pathways in cancer by Chinese medicine. *CANCER LETTERS*  
478 2:304-312. 10.1016/j.canlet.2010.07.015

479 Pan, H., Fu, X., and Huang, W. 2011. Molecular mechanism of liver cancer. *Anti-Cancer Agents*  
480 *in Medicinal Chemistry* 11:493-499.

481 Pan, Y., Ke, Z., Ye, H., Sun, L., Ding, X., Shen, Y., Zhang, R., and Yuan, J. 2019. Saikosaponin  
482 C exerts anti-HBV effects by attenuating HNF1 $\alpha$  and HNF4 $\alpha$  expression to suppress HBV  
483 pgRNA synthesis. *INFLAMMATION RESEARCH* 68:1025-1034. 10.1007/s00011-019-01284-2  
484 Fernández, F.P., Fondevila, F., Méndez, B. C.2019 Antitumor Effects of Quercetin in  
485 Hepatocarcinoma In Vitro and In Vivo Models: A Systematic Review. *Nutrient* 11.  
486 [10.3390/nu11122875](https://doi.org/10.3390/nu11122875)

487 Sandra, R., and Jean-Charles, N. 2020. Advances in molecular classification and precision  
488 oncology in hepatocellular carcinoma. *JOURNAL OF HEPATOLOGY* 72:215-229.

489 Shu, Z., He, W., Shahan, M., Guo, Z., Shu, J., Wu, T., Bian, X., Shar, A.H., Farag, M.R.,  
490 Alagawany, M., and Liu, C. 2018. Clarifying of the potential mechanism of Sinisan formula for  
491 treatment of chronic hepatitis by systems pharmacology method. *BIOMEDICINE &*  
492 *PHARMACOTHERAPY* 100:532-550. 10.1016/j.biopha.2018.02.047

493 Sukumar, U.K., Rajendran, J., Gambhir, S.S., Massoud, T.F., and Paulmurugan, R. 2020. SP94-  
494 Targeted Triblock Co-Polymer Nanoparticle Delivers Thymidine Kinase-p53-Nitroreductase  
495 Triple Therapeutic Gene and Restores Anticancer Function against Hepatocellular Carcinoma in  
496 vivo. *ACS Appl Mater Interfaces*. 10.1021/acsami.9b20071

497 Sun, J., Liu, H., Lv, C., Qin, J., and Wu, Y. 2019. Modification, Antitumor Activity, and  
498 Targeted PPAR $\gamma$  Study of 18 $\beta$ -Glycyrrhetic Acid, an Important Active Ingredient of Licorice.  
499 *JOURNAL OF AGRICULTURAL AND FOOD CHEMISTRY* 67:9643-9651.  
500 10.1021/acs.jafc.9b03442

501 Tao, W., Luo, X., Cui, B., Liang, D., Wang, C., Duan, Y., Li, X., Zhou, S., Zhao, M., Li, Y., He,  
502 Y., Wang, S., Kelley, K.W., Jiang, P., and Liu, Q. 2015. Practice of traditional Chinese medicine  
503 for psycho-behavioral intervention improves quality of life in cancer patients: A systematic  
504 review and meta-analysis. *Oncotarget* 6:39725. 10.18632/oncotarget.5388

505 Tsiambas E., Georgiannos SN., Salemis N., Alexopoulou D., Lambropoulou S., Dimo B. 2011.  
506 Significance of estrogen receptor 1 (ESR-1) gene imbalances in colon and hepatocellular  
507 carcinomas based on tissue microarrays analysis. *MEDICAL ONCOLOGY* 28: 934-940.  
508 [10.1007/s12032-010-9554-8](https://doi.org/10.1007/s12032-010-9554-8)

509 Villanueva, A. 2019. Hepatocellular Carcinoma. *The New England Journal of Medicine*  
510 380:1450-1462. 10.1056/NEJMra1713263

- 511 Wang R. E., Hunt C. R., Chen J., Taylor J. S. 2011. Biotinylated quercetin as an intrinsic  
512 photoaffinity proteomics probe for the identification of quercetin target proteins. *Bioorg. Med.*  
513 *Chem.* 19: 4710-20.
- 514 Xiang, Y., Zhang, Q., Wei, S., Huang, C., Li, Z., and Gao, Y. 2019. Paeoniflorin: a monoterpene  
515 glycoside from plants of Paeoniaceae family with diverse anticancer activities. *The Journal of*  
516 *pharmacy and pharmacology.* 10.1111/jphp.13204
- 517 Xiao-Cong, P., De, K., Jian-Song, F., and Ying, Z. 2018. Network pharmacology-based analysis  
518 of Chinese herbal Naodesheng formula for application to Alzheimer's disease. *Chinese Journal*  
519 *of Natural Medicines* 16:52-53.
- 520 Xiao-Ming, W., and Chun-Fu, W. 2015. Network pharmacology: A new approach to unveiling  
521 Traditional Chinese Medicine. *Chinese Journal of Natural Medicines* 13:1-2.
- 522 Xiaonian, Z., Daochuan, L., Zhengbao, Z., Wei, Z., and Wenxue, L. 2017. Persistent  
523 phosphorylation at specific H3 serine residues involved in chemical carcinogen-induced cell  
524 transformation. *MOLECULAR CARCINOGENESIS* 56:1449-1460.
- 525 Xue X., Zhang W., Huang C., Li Y., Yu H., Wang Y., Duan J., Ling Y. 2012. A novel  
526 chemometric method for the prediction of human oral bioavailability. *International Journal of*  
527 *Molecular Sciences* 13:6964-6982. [10.3390/ijms13066964](https://doi.org/10.3390/ijms13066964)
- 528 Yang, H., Li, Y., Shen, S., Gan, D., Han, C., Wu, J., and Wang, Z. 2019. Network  
529 Pharmacology-Based Investigation into the Mechanisms of Quyushengxin Formula for the  
530 Treatment of Ulcerative Colitis. *Evidence-based Complementary and Alternative Medicine*  
531 2019:22. 10.1155/2019/7870424
- 532 Zhang, R., Zhu, X., Bai, H., and Ning, K. 2019. Network Pharmacology Databases for  
533 Traditional Chinese Medicine: Review and Assessment. *Frontiers in Pharmacology* 10.  
534 10.3389/fphar.2019.00123
- 535 Zhao, S., Liu, Z., Wang, M., He, D., Liu, L., Shu, Y., Song, Z., Li, H., Liu, Y., and Lu, A. 2018.  
536 Anti-inflammatory effects of Zhishi and Zhiqiao revealed by network pharmacology integrated  
537 with molecular mechanism and metabolomics studies. *PHYTOMEDICINE* 50:61-72.  
538 10.1016/j.phymed.2018.09.184
- 539 Zhou, F., Wu, G., Cai, D., Xu, B., Yan, M., Ma, T., Guo, W., Zhang, W., Huang, X., Jia, X.,  
540 Yang, Y., Gao, F., Wang, P., and Lei, H. 2019. Synthesis and biological activity of

541 glycyrrhetic acid derivatives as antitumor agents. *EUROPEAN JOURNAL OF MEDICINAL*  
542 *CHEMISTRY* 178:623-635. 10.1016/j.ejmech.2019.06.029

543

544

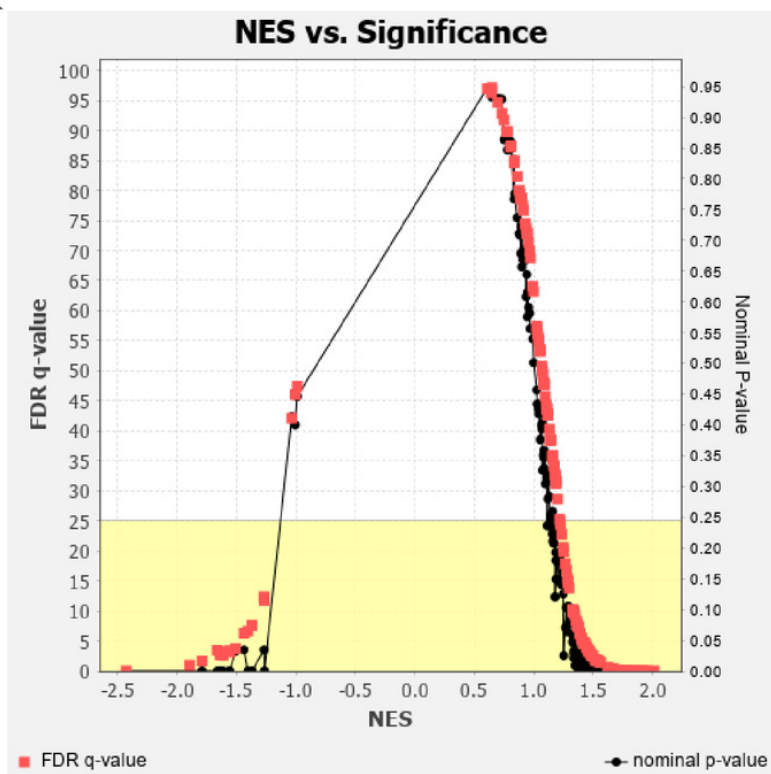
545

# Figure 1

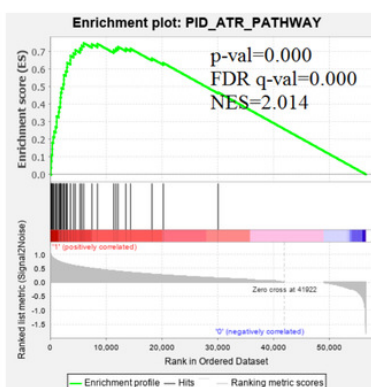
The results of GSEA enrichment analysis of stage III HCC genes from TCGA database.

(A) The normalized enrichment score (NES) and significance analysis of C2 curated gene sets (c2.cp.pid.v7.1) of GSEA; (B-I) The top 8 significantly enriched pathways (p value < 0.05 and FDR < 25%), namely: ARF pathway, ATM pathway, P53 REGULATION pathway, ATR pathway, AURORA A pathway, E2F pathway, FANCONI pathway and FOXM1 pathway.

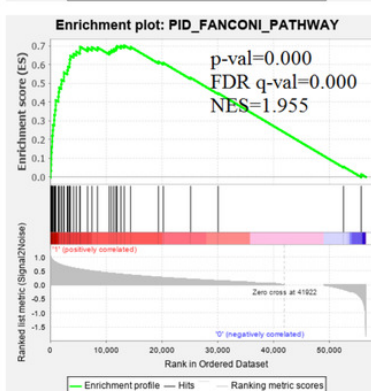
A



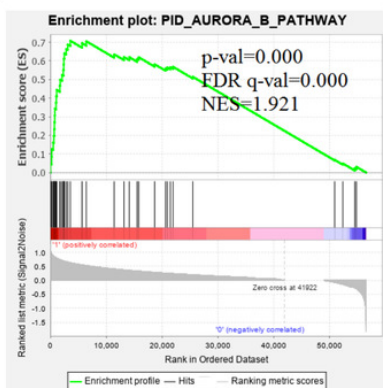
B



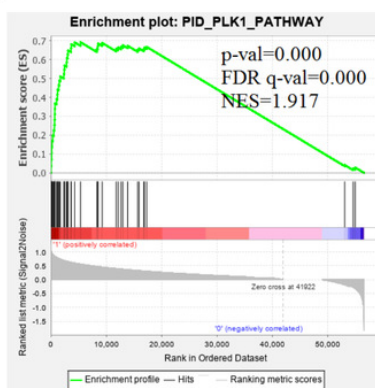
C



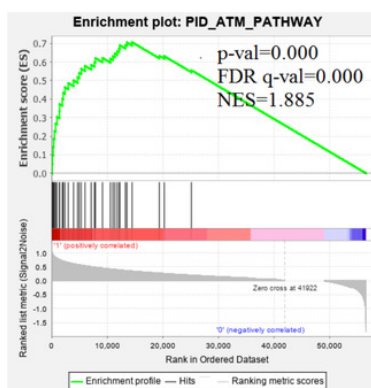
D



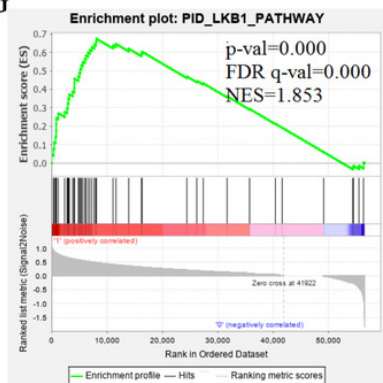
E



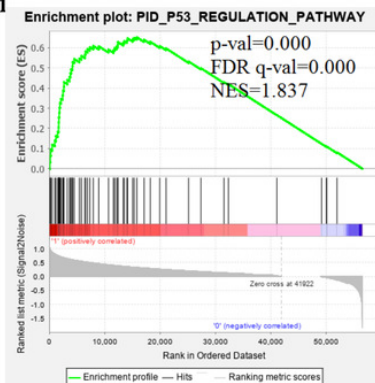
F



G



H



I

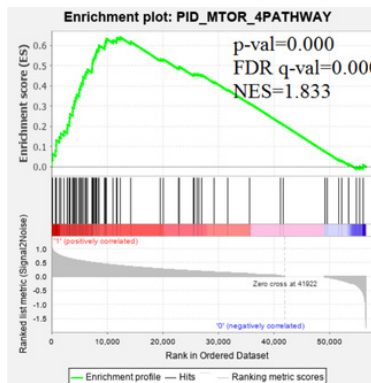
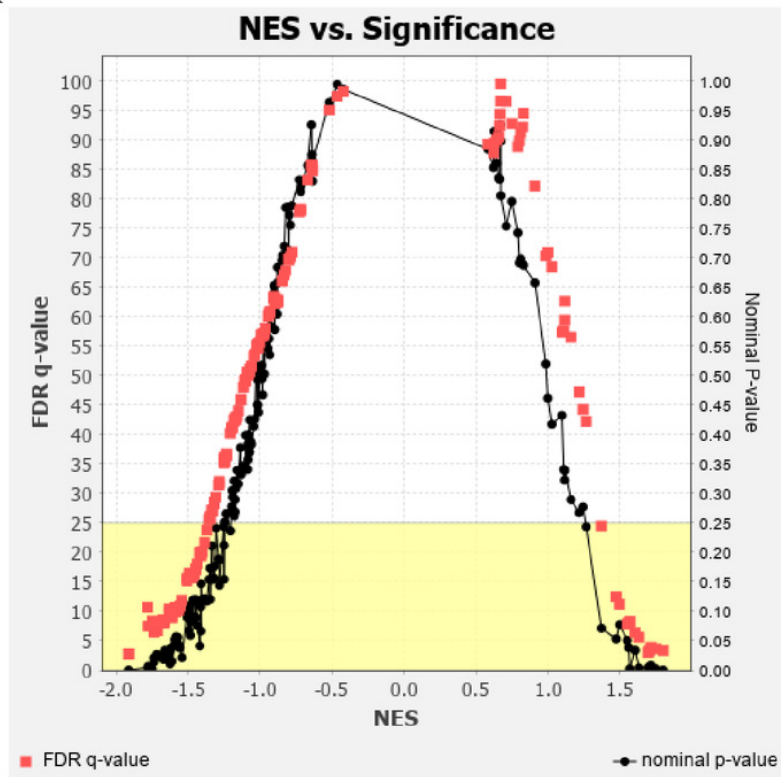


## Figure 2

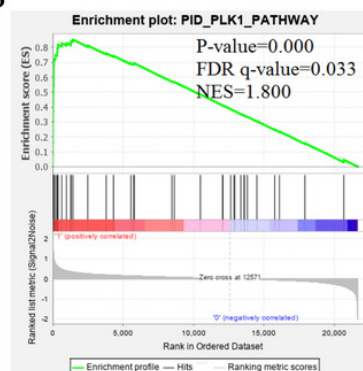
The results of GSEA enrichment analysis of stage III HCC genes from GEO database.

(A) The normalized enrichment score (NES) and significance analysis of C2 curated gene sets (c2.cp.pid.v7.1) of GSEA; (B-I) The top 8 significantly enriched pathways (p value < 0.05 and FDR < 25%), namely: ATR pathway, AURORA B pathway, DELTA NP63 pathway, FANCONI pathway, FOXM1 pathway, HIF1A pathway, P73 pathway and PLK1 pathway.

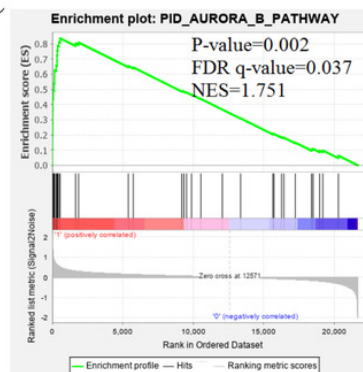
A



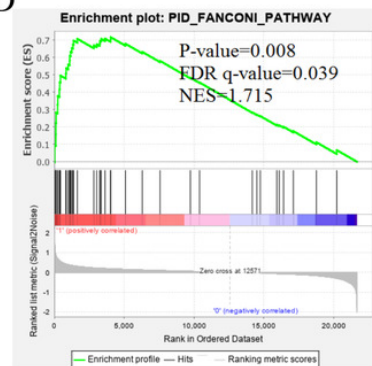
B



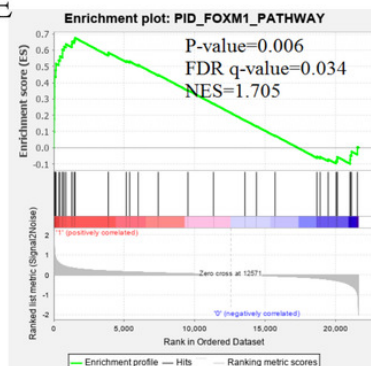
C



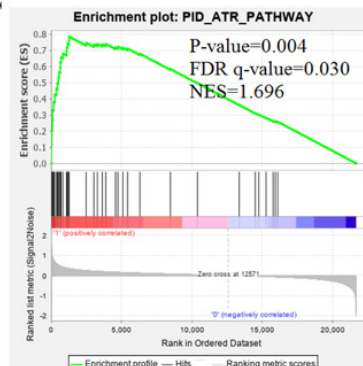
D



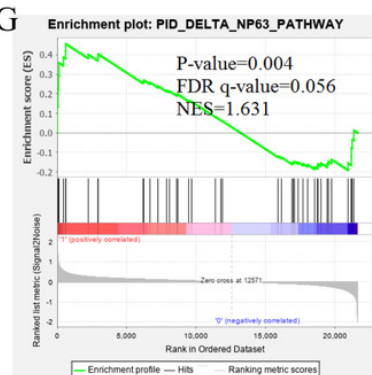
E



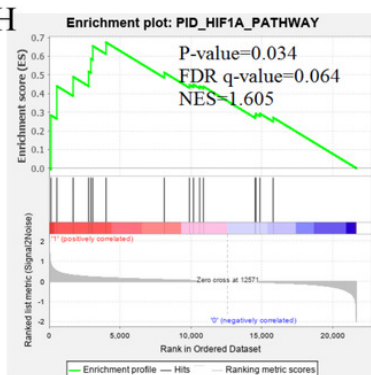
F



G



H



I

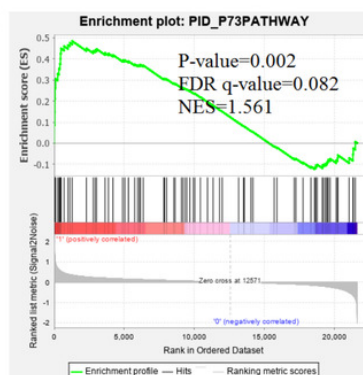


## Figure 3

The enriched pathway of GSEA analysis based on HCC targets from TCGA and GEO database

(A) GSEA enrichment analysis of stage III HCC genes from TCGA database. (B) GSEA enrichment analysis of stage III HCC genes from GEO database.

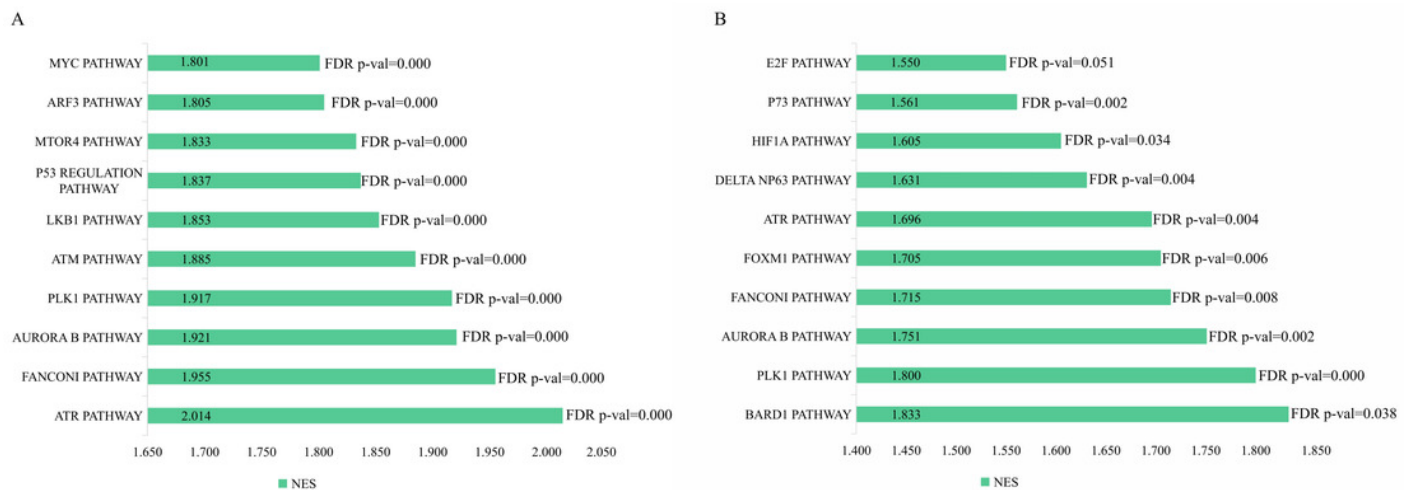


## Figure 4

The differentially expressed genes (DEGs) between normal and stage III HCC tissues.

The top genes were marked (A) DEGs from TCGA database; (B) DEGs from GEO database.

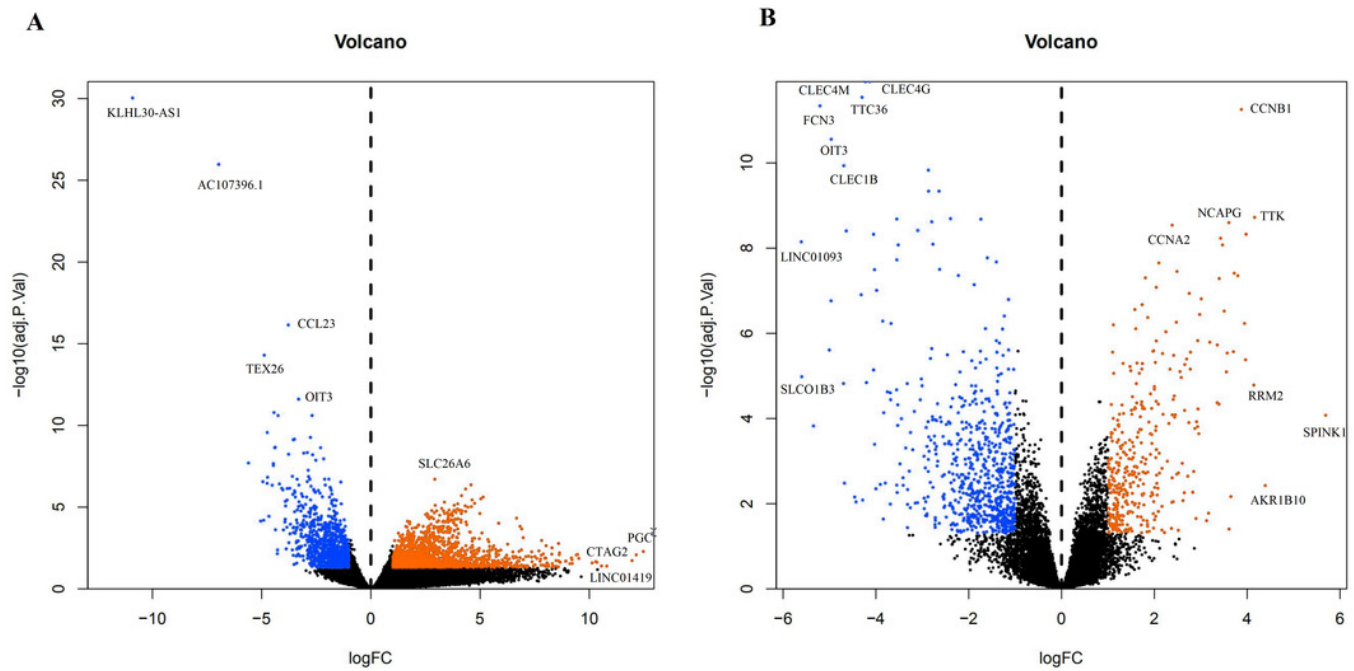




## Figure 6

The PPI network of the 64 targets of SiNiSan on stage III HCC.

The color of the nodes changing from blue to red represents the degree of the nodes changing from low to high.

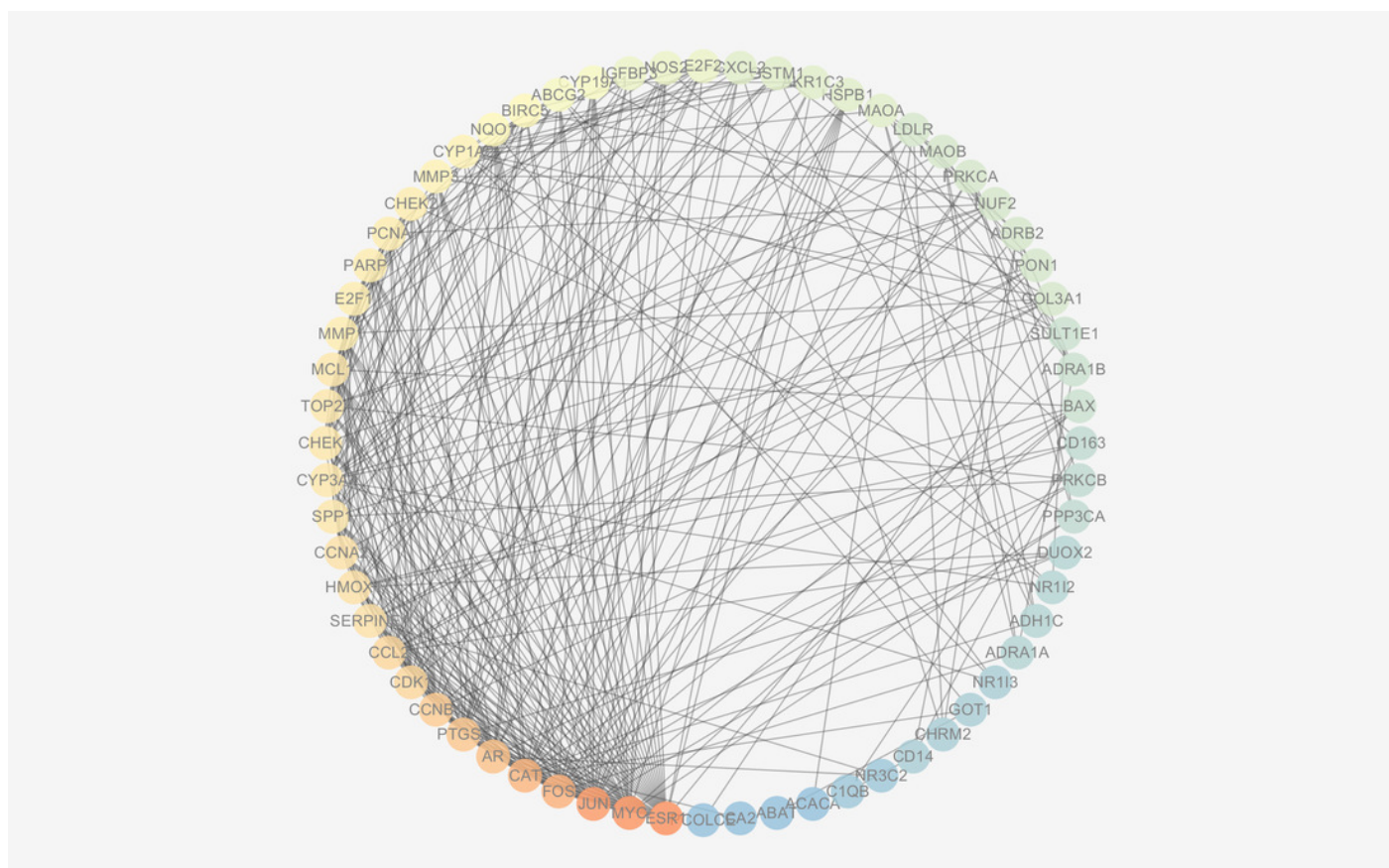


## Figure 7

The results of GO enrichment analysis of the 64 targets of SiNiSan on stage III HCC.

(A) the top 20 biological processes (BPs); (B) the top 20 cell compounds (CCs).

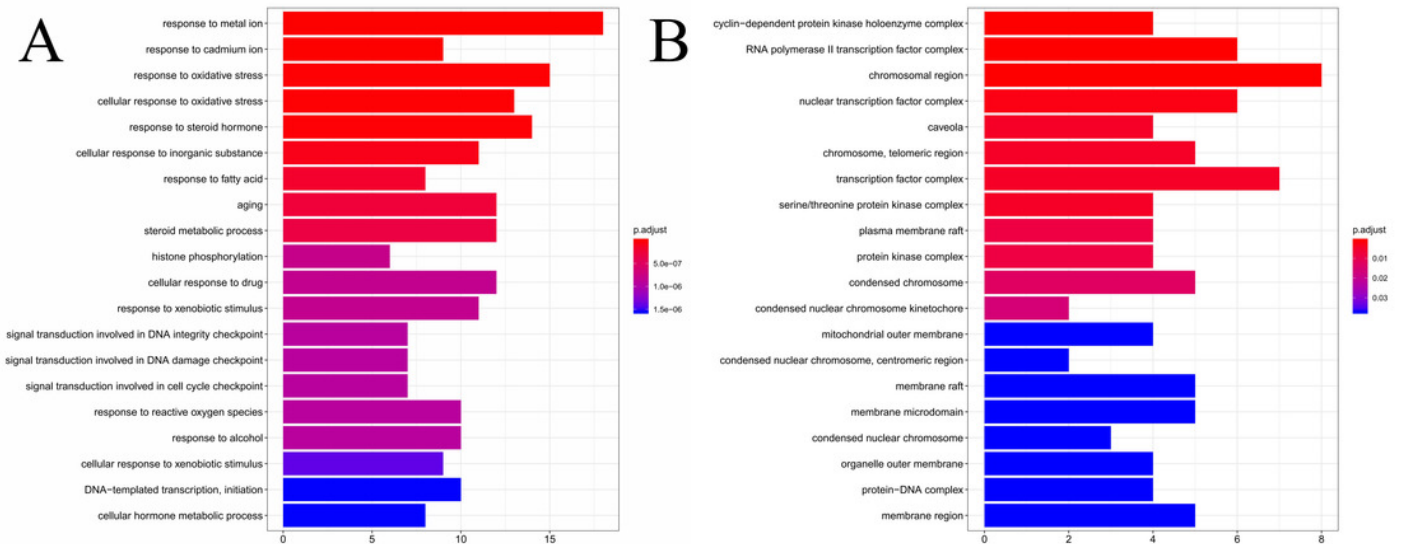


## Figure 8

The results of molecular docking between quercetin and genes CHEK2, BAX, AR, PTGS2.

In the picture, the blue molecule is quercetin, the pink is the amino acid residue where the target protein is docked with quercetin, and the yellow dotted line is the hydrogen bond.

(A)The molecular docking between quercetin ligand and CHEK2 macromolecule, the amino acid residue forming a hydrogen bond with quercetin is ARG-482; (B)The molecular docking between quercetin ligand and BAX macromolecule, the amino acid residue forming a hydrogen bond with quercetin is LYS-64 and SER-60; (C)The molecular docking between quercetin ligand and AR macromolecule, the amino acid residue forming a hydrogen bond with quercetin is GLU-308; (D)The molecular docking between quercetin ligand and PTGS2 macromolecule, the amino acid residue forming a hydrogen bond with quercetin is ASN-43.

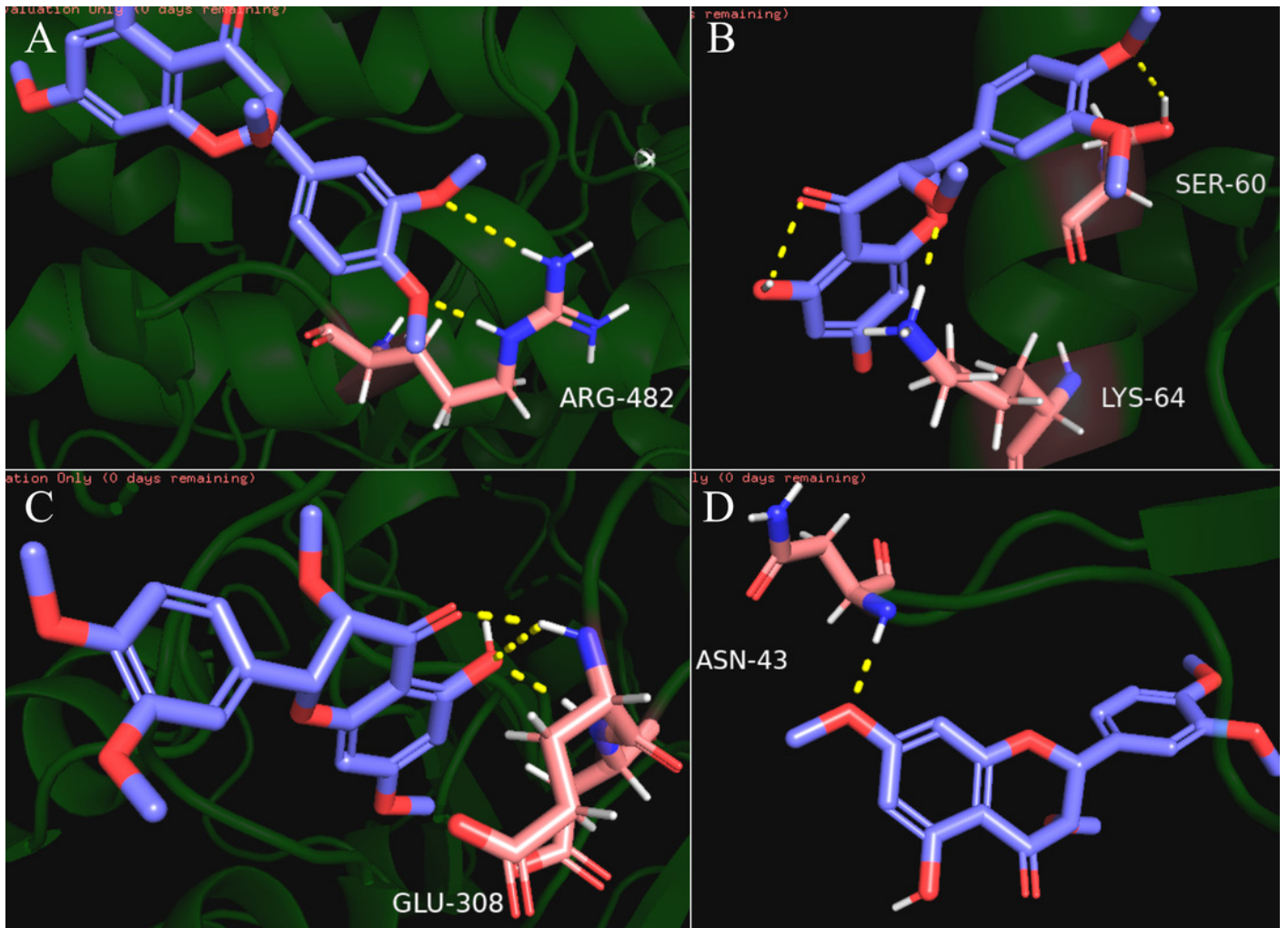


**Table 1** (on next page)

Active ingredients and parameters of SiNiSan.

ID	Herb	Compound	OB(%)	DL
MOL000358	Baishao	beta-sitosterol	36.91	0.75
MOL000492	Baishao	(+)-catechin	54.83	0.24
MOL001919	Baishao	(3S,5R,8R,9R,10S,14S)-3,17-dihydroxy-4,4,8,10,14-pentamethyl-2,3,5,6,7,9-hexahydro-1H-cyclopenta[a]phenanthrene-15,16-dione	43.56	0.53
MOL001924	Baishao	paeoniflorin	53.87	0.79
MOL000449	Chaihu	Stigmasterol	43.83	0.76
MOL000490	Chaihu	petunidin	30.05	0.31
MOL001645	Chaihu	Linoleyl acetate	42.1	0.2
MOL004598	Chaihu	3,5,6,7-tetramethoxy-2-(3,4,5-trimethoxyphenyl)chromone	31.97	0.59
MOL004609	Chaihu	Areapillin	48.96	0.41
MOL004653	Chaihu	(+)-Anomalin	46.06	0.66
MOL004718	Chaihu	$\alpha$ -spinasterol	42.98	0.76
MOL013187	Chaihu	Cubebin	57.13	0.64
MOL000239	Gancao	Jaranol	50.83	0.29
MOL000392	Gancao	formononetin	69.67	0.21
MOL000417	Gancao	Calycosin	47.75	0.24
MOL000497	Gancao	licochalconea	40.79	0.29
MOL000500	Gancao	Vestitol	74.66	0.21
MOL001484	Gancao	Inermine	75.18	0.54
MOL001792	Gancao	DFV	32.76	0.18
MOL002311	Gancao	Glycyrol	90.78	0.67

MOL002565	Gancao	Medicarpin	49.22	0.34
MOL003656	Gancao	Lupiwighteone	51.64	0.37
MOL003896	Gancao	7-Methoxy-2-methyl isoflavone	42.56	0.2
MOL004805	Gancao	(2S)-2-[4-hydroxy-3-(3-methylbut-2-enyl)phenyl]-8,8-dimethyl-2,3-dihydropyrano[2,3-f]chromen-4-one	31.79	0.72
MOL004806	Gancao	euchrenone	30.29	0.57
MOL004808	Gancao	glyasperin B	65.22	0.44
MOL004810	Gancao	glyasperin F	75.84	0.54
MOL004811	Gancao	Glyasperin C	45.56	0.4
MOL004814	Gancao	Isotrifoliol	31.94	0.42
MOL004815	Gancao	(E)-1-(2,4-dihydroxyphenyl)-3-(2,2-dimethylchromen-6-yl)prop-2-en-1-one	39.62	0.35
MOL004820	Gancao	kanzonols W	50.48	0.52
MOL004824	Gancao	(2S)-6-(2,4-dihydroxyphenyl)-2-(2-hydroxypropan-2-yl)-4-methoxy-2,3-dihydrofuro[3,2-g]chromen-7-one	60.25	0.63
MOL004827	Gancao	Semilicoisoflavone B	48.78	0.55
MOL004828	Gancao	Glepidotin A	44.72	0.35
MOL004829	Gancao	Glepidotin B	64.46	0.34
ID	Herb	Compound	OB(%)	DL
MOL004833	Gancao	Phaseolinisoflavan	32.01	0.45
MOL004835	Gancao	Glypallichalcone	61.6	0.19
MOL004838	Gancao	8-(6-hydroxy-2-benzofuranyl)-2,2-dimethyl-5-chromenol	58.44	0.38
MOL004841	Gancao	Licochalcone B	76.76	0.19
MOL004848	Gancao	licochalcone G	49.25	0.32

MOL004849	Gancao	3-(2,4-dihydroxyphenyl)-8-(1,1-dimethylprop-2-enyl)-7-hydroxy-5-methoxy-coumarin	59.62	0.43
MOL004855	Gancao	Licoricone	63.58	0.47
MOL004856	Gancao	Gancaonin A	51.08	0.4
MOL004857	Gancao	Gancaonin B	48.79	0.45
MOL004863	Gancao	3-(3,4-dihydroxyphenyl)-5,7-dihydroxy-8-(3-methylbut-2-enyl)chromone	66.37	0.41
MOL004864	Gancao	5,7-dihydroxy-3-(4-methoxyphenyl)-8-(3-methylbut-2-enyl)chromone	30.49	0.41
MOL004866	Gancao	2-(3,4-dihydroxyphenyl)-5,7-dihydroxy-6-(3-methylbut-2-enyl)chromone	44.15	0.41
MOL004879	Gancao	Glycyrin	52.61	0.47
MOL004882	Gancao	Licocoumarone	33.21	0.36
MOL004883	Gancao	Licoisoflavone	41.61	0.42
MOL004884	Gancao	Licoisoflavone B	38.93	0.55
MOL004885	Gancao	licoisoflavanone	52.47	0.54
MOL004891	Gancao	shinpterocarpin	80.3	0.73
MOL004898	Gancao	(E)-3-[3,4-dihydroxy-5-(3-methylbut-2-enyl)phenyl]-1-(2,4-dihydroxyphenyl)prop-2-en-1-one	46.27	0.31
MOL004903	Gancao	liquiritin	65.69	0.74
MOL004904	Gancao	licopyranocoumarin	80.36	0.65
MOL004907	Gancao	Glyzaglabrin	61.07	0.35
MOL004908	Gancao	Glabridin	53.25	0.47
MOL004910	Gancao	Glabranin	52.9	0.31

MOL004911	Gancao	Glabrene	46.27	0.44
MOL004912	Gancao	Glabrone	52.51	0.5
MOL004913	Gancao	1,3-dihydroxy-9-methoxy-6-benzofurano[3,2-c]chromenone	48.14	0.43
MOL004914	Gancao	1,3-dihydroxy-8,9-dimethoxy-6-benzofurano[3,2-c]chromenone	62.9	0.53
MOL004915	Gancao	Eurycarpin A	43.28	0.37
MOL004924	Gancao	(-)-Medicocarpin	40.99	0.95
MOL004935	Gancao	Sigmoidin-B	34.88	0.41
MOL004941	Gancao	(2R)-7-hydroxy-2-(4-hydroxyphenyl)chroman-4-one	71.12	0.18
MOL004945	Gancao	(2S)-7-hydroxy-2-(4-hydroxyphenyl)-8-(3-methylbut-2-enyl)chroman-4-one	36.57	0.32
MOL004948	Gancao	Isoglycyrol	44.7	0.84
ID	Herb	Compound	OB(%)	DL
MOL004949	Gancao	Isolicoflavonol	45.17	0.42
MOL004957	Gancao	HMO	38.37	0.21
MOL004959	Gancao	1-Methoxyphaseollidin	69.98	0.64
MOL004961	Gancao	Quercetin der.	46.45	0.33
MOL004966	Gancao	3'-Hydroxy-4'-O-Methylglabridin	43.71	0.57
MOL004974	Gancao	3'-Methoxyglabridin	46.16	0.57
MOL004978	Gancao	2-[(3R)-8,8-dimethyl-3,4-dihydro-2H-pyrano[6,5-f]chromen-3-yl]-5-methoxyphenol	36.21	0.52
MOL004980	Gancao	Inflacoumarin A	39.71	0.33
MOL004988	Gancao	Kanzonol F	32.47	0.89
MOL004989	Gancao	6-prenylated eriodictyol	39.22	0.41

MOL004990	Gancao	7,2',4'-trihydroxy-5-methoxy-3-arylcoumarin	83.71	0.27
MOL004991	Gancao	7-Acetoxy-2-methylisoflavone	38.92	0.26
MOL004993	Gancao	8-prenylated eriodictyol	53.79	0.4
MOL005000	Gancao	Gancaonin G	60.44	0.39
MOL005001	Gancao	Gancaonin H	50.1	0.78
MOL005003	Gancao	Licoagrocarpin	58.81	0.58
MOL005007	Gancao	Glyasperins M	72.67	0.59
MOL005008	Gancao	Glycyrrhiza flavonol A	41.28	0.6
MOL005012	Gancao	Licoagroisoflavone	57.28	0.49
MOL005016	Gancao	Odoratin	49.95	0.3
MOL005017	Gancao	Phaseol	78.77	0.58
MOL005018	Gancao	Xambioona	54.85	0.87
MOL005020	Gancao	dehydroglyasperins C	53.82	0.37
MOL000006	Zhishi	luteolin	36.16	0.25
MOL001798	Zhishi	neohesperidin_qt	71.17	0.27
MOL001803	Zhishi	Sinensetin	50.56	0.45
MOL001941	Zhishi	Ammidin	34.55	0.22
MOL002914	Zhishi	Eriodyctiol (flavanone)	41.35	0.24
MOL005100	Zhishi	5,7-dihydroxy-2-(3-hydroxy-4-methoxyphenyl)chroman-4-one	47.74	0.27
MOL005828	Zhishi	nobiletin	61.67	0.52
MOL005849	Zhishi	didymin	38.55	0.24
MOL007879	Zhishi	Tetramethoxyluteolin	43.68	0.37

MOL009053	Zhishi	4-[(2S,3R)-5-[(E)-3-hydroxyprop-1-enyl]-7-methoxy-3-methylol-2,3-dihydrobenzofuran-2-yl]-2-methoxy-phenol	50.76	0.39
MOL013277	Zhishi	Isosinensetin	51.15	0.44
MOL013279	Zhishi	5,7,4'-Trimethylapigenin	39.83	0.3
MOL013430	Zhishi	Prangenin	43.6	0.29
MOL013435	Zhishi	poncimarin	63.62	0.35
MOL013436	Zhishi	isoponcimarin	63.28	0.31
MOL013437	Zhishi	6-Methoxy auraptin	31.24	0.3
ID	Herb	Compound	OB(%)	DL
MOL004828	Gancao	Glepidotin A	44.72	0.35
MOL004829	Gancao	Glepidotin B	64.46	0.34
MOL004833	Gancao	Phaseolinisoflavan	32.01	0.45
MOL004835	Gancao	Glypallichalcone	61.6	0.19
MOL004838	Gancao	8-(6-hydroxy-2-benzofuranyl)-2,2-dimethyl-5-chromenol	58.44	0.38
MOL004841	Gancao	Licochalcone B	76.76	0.19
MOL004848	Gancao	licochalcone G	49.25	0.32
MOL004849	Gancao	3-(2,4-dihydroxyphenyl)-8-(1,1-dimethylprop-2-enyl)-7-hydroxy-5-methoxy-coumarin	59.62	0.43
MOL004855	Gancao	Licoricone	63.58	0.47
MOL004856	Gancao	Gancaonin A	51.08	0.4
MOL000098	Multi-herb	quercetin	46.43	0.28
MOL000354	Multi-herb	isorhamnetin	49.6	0.31
MOL000359	Multi-herb	sitosterol	36.91	0.75

---

MOL000422	Multi-herb	kaempferol	41.88	0.24
MOL004328	Multi-herb	naringenin	59.29	0.21

---



**Table 2** (on next page)

The results of KEGG pathway enrichment analysis of 64 intersection HCC genes.

ID	Description	pvalue	geneID
hsa04110	Cell cycle	4.70E-06	CDK1/CCNA2/CHEK1/MYC/CCNB1/CHEK2/E2F1/E2F2/PCNA
hsa04115	p53 signaling pathway	9.62E-06	BAX/CDK1/CHEK1/CCNB1/SERPIN1/CHEK2/IGFBP3
hsa00982	Drug metabolism - cytochrome P450	9.82E-05	CYP3A4/CYP1A2/GSTM1/ADH1C/MAOB/MAOA
hsa00140	Steroid hormone biosynthesis	0.000424164	CYP3A4/CYP1A2/AKR1C3/SULT1E1/CYP19A1
hsa00350	Tyrosine metabolism	0.000521784	ADH1C/MAOB/MAOA/GOT1
hsa01522	Endocrine resistance	0.000536494	BAX/JUN/ESR1/FOS/E2F1/E2F2
hsa00360	Phenylalanine metabolism	0.000695885	MAOB/MAOA/GOT1
hsa00380	Tryptophan metabolism	0.000945976	CYP1A2/CAT/MAOB/MAOA
hsa04020	Calcium signaling pathway	0.000947819	ADRA1A/CHRM2/ADRA1B/ADRB2/PRKCA/NOS2/PPP3CA/PRKCB
hsa00330	Arginine and proline metabolism	0.00182834	NOS2/MAOB/MAOA/GOT1
hsa04064	NF-kappa B signaling pathway	0.004651344	CD14/PTGS2/PRKCB/PARP1/CXCL2
hsa04066	HIF-1 signaling pathway	0.005678296	PRKCA/NOS2/HMOX1/PRKCB/SERPINE1
hsa01524	Platinum drug resistance	0.007222453	BAX/GSTM1/BIRC5/TOP2A
hsa00980	Metabolism of xenobiotics by cytochrome P450	0.008704905	CYP3A4/CYP1A2/GSTM1/ADH1C

**Table 3** (on next page)

The results of molecular docking between quercetin and AR, BAX, CHEK2, ESR1, NOS2, PTGS2.

Including binding energy, the inhibition constant, the total internal energy (V<sub>dw-hb-desolv</sub> + electrostatic energy) between the receptor and the ligand.

Component ligand	Target	PDB ID	Hbonding atoms of target	Hbinding energy (Kcal/mol)	Inhib constant	Vdw-hb-desolv + electrostatic energy (Kcal/mol)
Quercetin	AR	4WEV	GLU308:HN; ASP309:HN	-4.24	775.54 uM	-6.04
Quercetin	PTGS2	5KIR	ASN43:H	-4.11	976.06 uM	-5.9
Quercetin	PTGS2	5KIR	GLY66:H	-3.93	1.32 mM	-5.72
Quercetin	AR	2Q7K	ARG788:HH11; HIS789:HD1; GLN792:HE22	-3.36	3.45 mM	-5.14
Quercetin	CHEK2	2CN8	ARG474:HH22	-3.36	3.44 mM	-5.15
Quercetin	PTGS2	5KIR	ARG77:HE; ARG77:HH11	-3.2	6.28 mM	-4.79
Quercetin	PTGS2	5KIR	ARG44:HE; CYS47:H	-3.19	4.55 mM	-4.99
Quercetin	NOS2	5XN3	GLU219:HN	-3.17	4.78 mM	-4.96
Quercetin	PTGS2	5KIR	LYS83:HZ1	-3.11	3.72 mM	-5.1
Quercetin	AR	2Q7K	ARG788:HH11; ARG788:HH21; HIS789:HD1; GLN792:HE22	-3.05	5.8 mM	-4.85
Quercetin	CHEK2	4A9U	ARG482:HE	-3.05	5.78 mM	-4.84
Quercetin	CHEK2	2CN8	LYS444:HZ1	-3.04	5.86 mM	-4.84
Quercetin	BAX	4BD7	SER60:HG; LYS64:HZ3	-3.00	3.83 mM	-5.09
Quercetin	PTGS2	5KIR	HIS90:HD1	-2.91	6.7 mM	-4.75

---

Quercetin	CHEK2	2CN8	LYS464:HZ2	-2.78	9.17 mM	-4.57
Quercetin	AR	5BXJ	ARG39:HH12; HIS56:HE2	-2.23	23.17 mM	-4.02
Quercetin	AR	5BXJ	ARG39:HH22; LYS99:HZ1	-2.19	24.99 mM	-3.98
Quercetin	NOS2	4NOS	LYS123:HZ3	-1.68	58.96 mM	-3.47
Quercetin	BAX	4BD6	LYS119:HZ1	-1.67	59.9 mM	-3.46
Quercetin	ESR1	6KN5	LYS996:HZ1	-1.64	63.15 mM	-3.43
Quercetin	BAX	4BD6	SER72: HG	-1.59	68.29 mM	-3.38
Quercetin	ESR1	4XI3	LYS467:HZ1	-1.59	68.65 mM	-3.53

---

1

2